Pressure dependence of the upper critical field of MgB_2 and of YNi_2B_2C

H. Suderow,[1] V. G. Tissen,[2] J. P. Brison,[3] J. L. Martínez,[2] S. Vieira,[1] P. Lejay,[3] S. Lee,[4] and S. Tajima[4]
[1]*Laboratorio de Bajas Temperaturas, Dpto Física Materia Condensada, Instituto de Ciencia de Materiales Nicolás Cabrera, Universidad Autónoma de Madrid, 28049 Madrid, Spain*
[2]*Instituto de Ciencia de Materiales de Madrid, Consejo Superior de Investigaciones Científicas, 28049 Madrid, Spain*
[3]*Centre des Recherches sur les Très Basses Températures CNRS, BP 166, 38042 Grenoble Cedex 9, France*
[4]*Superconductivity Research Laboratory, ISTEC, 1-10-13, Shinonome, Koto-ku, Tokyo, 135-0062 Japan*
(Received 21 April 2004; revised manuscript received 17 June 2004; published 29 October 2004)

We present measurements of $H_{c2}(T)$ under pressure in MgB_2 and in YNi_2B_2C. The changes in the shape of $H_{c2}(T)$ are interpreted within current models and show the evolution of the main Fermi surface velocities v_F and electron-phonon coupling parameters λ with pressure. In MgB_2 the electron-phonon coupling strength of the nearly two-dimensional σ band, responsible for the high critical temperature, is more affected by pressure than the π band coupling, and the hole doping of the σ band decreases. In YNi_2B_2C, the peculiar positive curvature of $H_{c2}(T)$ is weakened by pressure.

DOI: 10.1103/PhysRevB.70.134518 PACS number(s): 74.62.Fj, 74.70.Ad, 74.70.Dd, 74.25.Op

I. INTRODUCTION

Recent advances in the synthesis and study of new materials have shown that a highly nonuniform electron-phonon coupling over the Fermi surface can lead to many new, and unexpected, superconducting properties.[1] In MgB_2, which superconducts at $T_c = 40$ K,[2] the electron-phonon coupling is very different in the two sets of bands of the Fermi surface, the quasi-two-dimensional σ bands, which strongly couple to the in-plane high-energy E_{2g} B-B phonon mode, and the three-dimensional π bands, leading to the much-discussed two-band superconductivity.[3–8] Several new effects are currently under discussion, such as, e.g., possible internal modes and soliton structures.[9,10] In the nonmagnetic nickel borocarbide superconductor YNi_2B_2C [with $T_c = 15.5$ *K* (Ref. 11)] the superconducting gap is highly anisotropic and vanishes on points or lines of the Fermi surface.[12–17] Superconducting electron tunneling spectroscopy,[17] together with photoemission and point contact experiments,[14,18] demonstrated the importance for the pairing interaction of a low-energy (4 meV) phonon mode, softened by a nesting feature of the Fermi surface,[19] a phenomenon previously observed in neutron scattering experiments.[20]

The underlying physical properties of MgB_2 and YNi_2B_2C are clearly different, and they represent interesting limiting behaviors of electron-phonon-coupled superconductors. MgB_2 is the most clear-cut example of two-band superconductivity, and YNi_2B_2C has the highest reported anisotropy of the superconducting gap.[15] It has been found that in both compounds, the temperature dependence of the upper critical field $H_{c2}(T)$ significantly deviates from the linear behavior expected at low fields within isotropic, single-band, BCS *s*-wave theory. Instead, the shape of $H_{c2}(T)$ shows a positive curvature (PC), which is a direct consequence of the presence of two well-differentiated subgroups of electrons on the Fermi surface. The Fermi velocities and electron-phonon coupling parameters of these subgroups of electrons are obtained by fitting the shape of $H_{c2}(T)$ within the effective two-band model described in Refs. 12 and 21 and in Appendix A.

Studying the changes induced by variations in the volume of the unit cell on the different Fermi surface and electron-phonon coupling parameters is clearly of paramount importance to get a full understanding of this intriguing kind of superconductors, and $H_{c2}(T)$ under pressure appears as a valuable tool to do so. As a matter of fact, the pressure dependence of $H_{c2}(T)$ has been previously used to obtain microscopic information of the Fermi surface and coupling parameters of other kinds of superconducting materials.[22] However, although several studies address $H_{c2}(T)$ at ambient pressure in MgB_2 and in YNi_2B_2C,[12,21,23–25] to the best of our knowledge, no previous measurements of the evolution of $H_{c2}(T)$ under pressure are available. Note that several groups have systematically studied the effect of chemical pressure on the upper critical field of MgB_2.[26,27] In that case scattering effects dominate the observed behavior, leading to an increase of the interband and/or intraband coupling, which smears out the differences in the electronic properties and in the coupling to the phonon modes between the subgroups of electrons found in the pure compounds.[28] The goal of this work is to obtain information about the changes induced by pressure on the different parts of the Fermi surface by measuring and analyzing the pressure dependence of $H_{c2}(T)$ in MgB_2 and YNi_2B_2C.

II. EXPERIMENT

The single crystals of MgB_2 were grown as described in Ref. 29 and the ones of YNi_2B_2C in an image furnace.[17] Small samples of size $0.12 \times 0.12 \times 0.03$ mm^3, cut from mother crystals, were loaded into a hole in NiMo-alloy gasket positioned between two diamond anvils with 0.7 mm culet diameter. The pressure in the cell was determined by the ruby fluorescence method.

A susceptometer was designed to obtain the largest signal-to-noise ratio, with a pickup coil wounded very close to the sample space. Anvils were glued to the sapphire backing plates in order to reduce the inductive coupling between coil systems used for ac susceptibility measurements and the

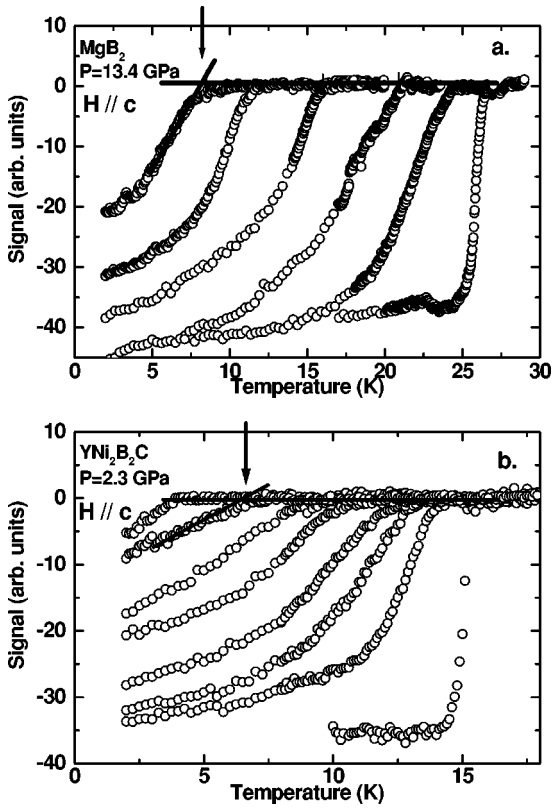

FIG. 1. The temperature dependence of the ac susceptibility is shown for several magnetic fields at 13.4 GPa in MgB_2 [from right to left in (a), 0, 0.1, 0.3, 0.7, 1.0, 1.2 T] and at 2.3 GPa in YNi_2B_2C [from right to left in (b), 0, 0.1, 0.3, 0.5, 1.0, 2.0, 3.0, 5.0 T]. Lines and arrows graphically demonstrate the way we extract the critical temperature (onset criterion; see also text). This series of curves is a representative example of the transitions measured to obtain the $H_{c2}(T)$ data shown in Figs. 2 (MgB_2) and 4 (YNi_2B_2C).

body of a diamond anvil cell made of Cu-Be alloy. The secondary coils of two identical coil systems were connected in opposition, thus forming a bridge. The measuring coil system is mounted symmetrically around the anvils and the reference system is placed nearby. After additional compensation by means of an attenuator and a phase shifter the total signal is detected with a lock-in amplifier.

Using this susceptometer, we measured the ac susceptibility as a function of the temperature (down to 2 K) at different magnetic fields (up to 9 T) for several fixed pressures in each compound. The magnetic field was always applied perpendicular to the basal plane of the crystallographic structure. The critical temperature was determined the onset of the superconducting transition curves, which was defined as the intersection of two tangents, one to the flat portion of the curve above and the second to the steepest variation in the signal below superconducting transition, as shown by the lines in Figs. 1(a) and 1(b). In these figures we show a representative example of the temperature dependence of the susceptibility around several superconducting transitions, measured at different magnetic fields and at 13.4 GPa in MgB_2 and 2.3 GPa in YNi_2B_2C. From the dependence of the critical temperature as a function of the magnetic field at each pressure, we obtain the data shown in Figs. 2 and 4 and discussed in the rest of the paper.

On the other hand, we use a methanol-ethanol mixture as a pressure-transmitting medium, which is thought to give quasi-hydrostatic-pressure conditions. It is important to emphasize that previous measurements of $T_c(P)$ at zero magnetic field in hydrostatic conditions (with helium as a pressure-transmitting medium; see, e.g. Refs. 30 and 31 and references therein), made in MgB_2, agree well with the data presented here. Hence, we can exclude that the eventual deviations from hydrostatic conditions influence the results obtained here.

TABLE I. Parameters used for the ambient pressure fits. We have taken $\mu^*=0.1$ and a mean phonon frequency of $\theta=404$ K for MgB_2 and $\theta=248=$K for YNi_2B_2C. All parameters are similar to the ones used in previous work (Refs. 12 and 21). Slight differences arise from a simpler choice of the matrix of strong-coupling parameters (only two different values) describing the coupling anisotropy. In the case of YNi_2B_2C, our parameters agree well with the tunneling spectroscopy experiments of Ref. 17. For MgB_2, $\lambda_\sigma=\lambda_1$, $\lambda_\pi=\lambda_2=\lambda_{\pi\sigma}=\lambda_{12}=\lambda_{\sigma\pi}=\lambda_{21}$, and $v_\sigma=v_{F1}$, $v_\pi=v_{F2}$.

	λ_1	λ_2	v_{F1}	v_{F2}
MgB_2	1.1	0.35	0.29×10^6 m/s	0.9×10^6 m/s
YNi_2B_2C	0.84	0.27	0.059×10^6 m/s	0.7×10^6 m/s

III. RESULTS AND DISCUSSION

To interpret our data, we follow the microscopic model of Refs. 12 and 21, which numerically linearizes the equations for $H_{c2}(T)$ obtained from Eliashberg theory[32] (see the Appendix). The main change of $H_{c2}(T)$ under pressure occurs in the form of the PC and the value of $H_{c2}(T=0\ \mathrm{K})$, which are uniquely determined by the values of the coupling strengths

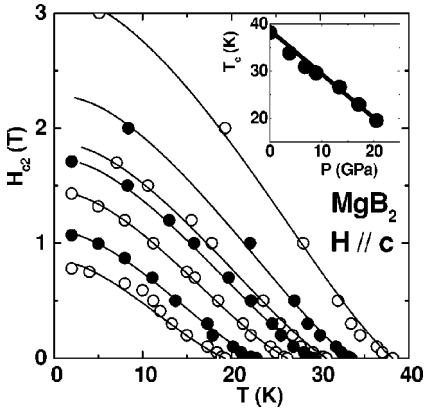

FIG. 2. Temperature dependence of the upper critical field under hydrostatic pressure of MgB_2 at, from top to bottom, ambient pressure 3.8, 6.8, 8.9, 13.4, 17.1, and 20.5 GPa. The magnetic field was applied along the c axis. The solid lines are fits discussed in the text. The inset shows the pressure dependence of the critical temperature obtained here (points). We obtain $dT_c/dP=-1.1$ K/GPa (line), in agreement with previous work in high-quality single-crystalline samples using helium as a pressure transmitting medium (Refs. 30 and 31).

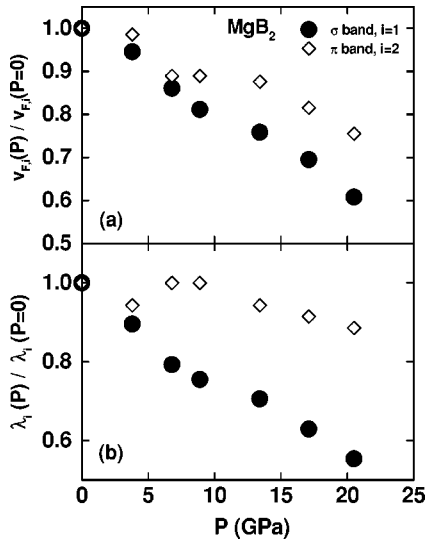

FIG. 3. Pressure dependence of the parameters obtained from the fits of Fig. 1 in MgB_2, normalized to their ambient pressure values (Table I). Solid circles represent the data for the σ bands and open diamonds represent data for the π bands. The electron-phonon coupling parameter λ (b) decreases with pressure, together with the Fermi velocities $v_{F1,F2}=v_{\sigma,\pi}$ for both bands (a). Note that λ_σ decreases much faster with pressure than λ_π (b).

λ_1 and λ_2 and Fermi velocities v_{F1} and v_{F2} of the different subgroups of electrons used to model the Fermi surface.[12] Here, we take for the interband coupling constants $\lambda_{12}=\lambda_{21}=\lambda_2$. In fact, the values found in the literature, λ_{12} and λ_{21}, are indeed close to λ_2,[12,21] and they show the same pressure dependences, if left as free parameters, as λ_2. Other parameters of the model—the Coulomb pseudopotential and a mean phonon frequency—do not affect the PC and form of $H_{c2}(T)$, and we therefore leave them unchanged (see Table I).

A. Upper critical field under pressure of MgB_2

The temperature dependence of the upper critical field of MgB_2 up to 20.5 GPa is shown in Fig. 2. We could not find any previous $H_{c2}(T,P)$ data under pressure, although, as already noted, $T_c(P,H=0)$ and $H_{c2}(T,P=0)$ have been thoroughly studied in Refs. 23–25, 30, 31, 33, and 34 and agree well with our data. More recently, a broadening of the transition under magnetic fields has been discussed in terms of fluctuations in Ref. 35. However, it appears to depend on the volume of the samples.

The critical temperature drops by a factor of 2 at 20.5 GPa and $H_{c2}(T=0\ \mathrm{K})$ by a factor of 4. The shape of $H_{c2}(T)$ changes by increasing pressure. The PC is always observed, although it appears to be slightly weakened by pressure. More detailed information is found by fitting the data (lines in Fig. 2) and following the evolution of the most important parameters, as shown in Fig. 3. The Fermi velocities [Fig. 3(a)] decrease for both sets of bands under pressure. The slightly stronger decrease of $v_{F\sigma}$ reflects the stronger pressure dependence of the band structure of this subgroup of electrons. The dispersion relation can be taken to be roughly quadratical in the basal plane, as the Fermi level cuts these bands near their top,[4,7] so that the Fermi velocity $v_{F\sigma}$ is approximately proportional to the radius of the σ sheets. Hence, the decrease observed here shows the continuous shrinking of the volume of the σ sheet under pressure. As emphasized in early band structure calculations on MgB_2 and related isoelectronic systems,[4] the layer of Mg^{2+} ions causes charge transfer from the σ to the π bands, doping with holes the σ bands, which strongly contribute to the density of states at the Fermi level due to their two dimensionality. Our data show how pressure reduces the doping and the σ-band density of states. This reduction appears to affect mainly the electron-phonon coupling in the σ bands [Fig. 3(b)]. As a matter of fact, previous estimations of the pressure effect on the overall coupling constant λ, based on the $T_c(P)$ measurements,[30,33] agree with the pressure dependence of λ_σ found here. Hence, the overall decrease in the electron-phonon coupling under pressure does not occur over the whole Fermi surface, but must be associated with a loss of electron-phonon coupling mainly in the σ bands, which is ultimately responsible for the decrease of $T_c(P)$.

On the other hand, we should also emphasize that the high-energy E_{2g} phonon mode, to which the σ-band electrons mainly couple, has been shown by Raman scattering measurements to stiffen under pressure, increasing its frequency by about 30% at 20 GPa.[31,33] Correspondingly, λ_σ decreases, as shown here in Fig. 3(b), because the hole doping of the σ bands, achieved through the ionic layered character of MgB_2, is gradually lost. Note also that previous experiments have identified a kink in $T_c(P)$ at 20 GPa, which has been attributed to an electronic topological transition, corresponding to one of the two σ sheets moving below the Fermi level at 20 GPa.[30,33,36] The decrease of $v_{F\sigma}$ observed here shows the pressure-induced filling of the σ bands and agrees well with this scenario.

B. Upper critical field under pressure of YNi_2B_2C

The pressure dependence of the critical temperature and upper critical field of YNi_2B_2C is shown in Fig. 4. Previous $T_c(P)$ measurements were done at zero field[37] and stopped at a much lower pressure (3 GPa), so that the decrease measured here most clearly above 3 GPa (inset of Fig. 4) could not be observed. $H_{c2}(T)$ at ambient pressure is in excellent agreement with previous work and shows the extreme PC discussed in Ref. 12. Remarkably, while the critical temperature is suppressed by a factor of 2 at 10 GPa, the zero-temperature extrapolation of the upper critical field drops by an order of magnitude. In addition, the PC in $H_{c2}(T)$ is also suppressed by pressure. The best fit to the data is shown as lines in Fig. 4. At ambient pressure, we obtain the parameters summarized in Table I. Their evolution as a function of pressure is shown in Fig. 5. Note that the electron-phonon coupling parameters λ_1 and λ_2 drop both continuously with pressure [Fig. 5(b)] in approximately the same way. However, the changes in the Fermi velocity occur mainly in the subgroup of electrons with strongest coupling [v_{F1}, Fig. 5(a)], evidencing an increase of the volume of the corresponding part of the Fermi surface.

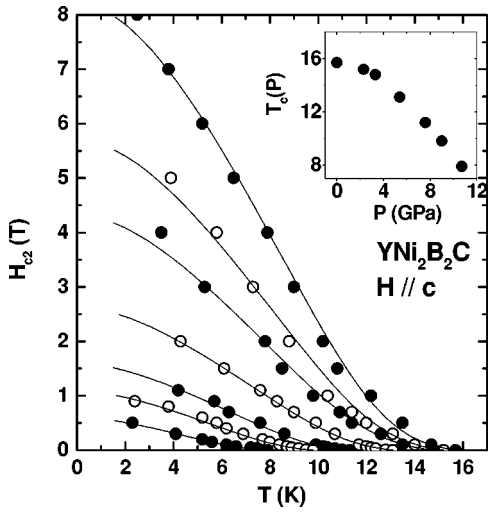

FIG. 4. The temperature dependence of the upper critical field of the Ni borocarbide superconductor YNi_2B_2C at, from top to bottom, ambient pressure 2.3, 3.3, 5.4, 7.6, 9.0, and 11.7 GPa together with the fits to the theory (solid lines) explained in the text. The inset shows the pressure dependence of the zero-field critical temperature.

At zero pressure, the Fermi surface nesting feature found in Ref. 19 leads to a significant softening of an acoustic phonon mode down to about 4 meV. The corresponding strong-coupling feature has been observed in tunneling spectroscopy, and an electron-phonon coupling parameter λ between 0.5 and 0.8, of the same order as the one used here for λ_1 at ambient pressure (Table I), has been obtained.[17] The decrease in the electron-phonon coupling under pressure shown in Fig. 5(b) should be related to the hardening of this mode and the concomitant disappearance of the Fermi surface nesting feature. This must be accompanied by an increase of the volume of the corresponding part of the Fermi surface, explaining the increase of v_{F1} observed here [Fig. 5(a)]. The importance of band structure effects in understanding the microscopic origin for the peculiar superconducting properties of YNi_2B_2C is evidenced by our data.

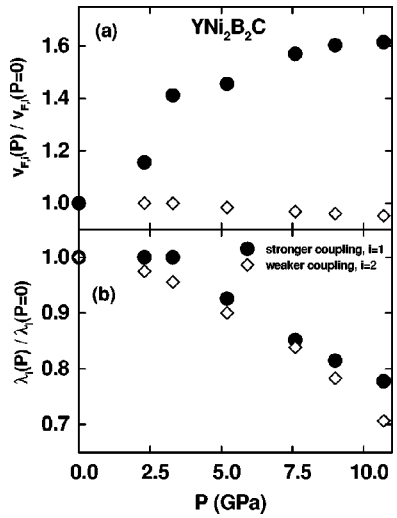

FIG. 5. The pressure dependence of the Fermi surface velocities (a) and electron-phonon coupling parameters (b) for both subgroup of electrons is shown as a function of pressure in YNi_2B_2C. They are normalized to their ambient pressure values (see Table I). The subgroup of electrons corresponding to the strongest-coupling part of the Fermi surface increases its Fermi velocity v_{F1} (a), and the electron-phonon coupling (b) is weakened under pressure.

IV. SUMMARY AND CONCLUSION

In summary, we have found that the evolution of $H_{c2}(T)$ under pressure in MgB_2 and YNi_2B_2C reflects the changes occurring in the band structure and electron-phonon coupling of the different subgroups of electrons on the Fermi surface. In the two-band superconductor MgB_2, the electron-phonon coupling in the σ band, responsible for its high critical temperature, is strongly affected by pressure through the reduction of the σ-band hole doping. In YNi_2B_2C, the critical temperature decreases continuously with pressure, together with the electron-phonon coupling parameters in both subgroups of electrons. $H_{c2}(T=0\ \mathrm{K})$ dramatically decreases under pressure, and, at the same time, the peculiar PC curvature of $H_{c2}(T)$ is weakened, showing the pressure-induced increase in the volume of the Fermi surface part corresponding to the strong-coupling subgroup of electrons.

ACKNOWLEDGMENTS

We specially acknowledge discussions and help of P.C. Canfield. We are also grateful to F. Guinea and A. Levanyuk and for receiving support from the ESF program VORTEX, from the MCyT (Spain, Grant Nos. MAT-2001-1281-C02-0, MAT-2002-1329 and SAB2000-039), and from the Comunidad Autónoma de Madrid (Grant No. 07N/0053/2002, Spain). This work was partially supported by the New Energy and Industrial Technology Development Organization (NEDO) as the Collaborative Research and Development of Fundamental Technologies for Superconductivity Applications. The Laboratorio de Bajas Temperaturas is associated to the ICMM of the CSIC.

APPENDIX

Equations for two-band superconductors have been given by numerous authors.[12,32] For the sake of completeness, we give here the linearized gap equations under magnetic field, for a superconductor in the clean limit (negligible impurity scattering), as can be found in Ref. 12 [with corrections of typographical mistakes of a factor of 2 in the Matsubara frequency and definition of $\lambda_{i,j}(n)$]. In the following, i and j are the band indices, $\alpha_{i,j}F(\omega)$ is the density of interactions from band i to j (involving diffusion from band i to j), v_{Fi} is the Fermi velocity of band i, and H_{c2} is the upper critical field:

$$\tilde{\Delta}_i(n) = \pi T \sum_{j,m} [\lambda_{i,j}(m-n) - \mu^* \delta_{i,j}\theta(\omega_c - |\omega_m|)] \times \chi_j(m)\tilde{\Delta}_j(m)(\omega_m),$$

$$\tilde{\omega}_i(n) = \omega_n + \pi T \sum_{j,m} [\lambda_{i,j}(m-n)]\mathrm{sgn}(\omega_m),$$

$$\chi_i(n) = (2/\sqrt{\beta_i}) \int_0^\infty dq \exp(-q^2) \times \tan^{-1}\left\{ \frac{q\sqrt{\beta_i}}{[|\tilde{\omega}_i(n)| + i\mu_B H_{c2}\mathrm{sgn}(\omega_n)]} \right\}, \quad \text{(A1)}$$

with

$$\beta_i = \pi H_{c2} v_{Fi}^2/(2\phi_0),\ \omega_n = \pi T(2n+1),$$

$$\lambda_{i,j}(n-m) = 2\int_0^\infty d\omega \alpha_{i,j}^2 \omega \frac{F(\omega)}{\omega^2 + (\omega_n - \omega_m)^2}.$$

The value of H_{c2} is given by the largest set of values of β_i yielding a nontrivial solution of Eq. (A1).

We have used in addition an Einstein spectrum for the density of interactions:

$$\alpha_{i,j}(\omega)F(\omega) = \frac{\lambda_{i,j}\Omega}{2}\delta(\omega - \Omega), \quad \text{(A2)}$$

introducing a characteristic energy scale Ω. In the calculations, we find $\Omega \approx 21$ K: let us note that this value of Ω cannot be determined by the fit of H_{c2} only: it depends directly of the absolute value of the $\lambda_{i,j}$ whereas the shape of H_{c2} is controlled only by the relative size of the $\lambda_{i,j}$ (as long as they are not too large). The cutoff parameter ω_c in Eqs. (A1) is taken to 10Ω, and the infinite system of equations (A1) has been truncated at each temperature when $|\omega_n|$ reaches ω_c.

Note also that bare Fermi velocities enter the above equations and that renormalized Fermi velocities $v_{Fi}^* = v_{Fi}/(1 + \Sigma_j \lambda_{i,j})$ should be used for comparison to specific heat or de Haas–van Alphen measurements.[38]

[1] B. H. Brandow, Philos. Mag. **83**, 2487 (2003).
[2] J. Nagamatsu *et al.*, Nature (London) **410**, 63 (2001).
[3] A. Y. Liu, I. I. Mazin, and J. Kortus, Phys. Rev. Lett. **87**, 087005 (2001).
[4] J. M. An and W. E. Pickett, Phys. Rev. Lett. **86**, 4366 (2001).
[5] H. J. Choi, D. Roundry, H. Sun, M. L. Cohen, and S. G. Louie, Nature (London) **418**, 758 (2002).
[6] G. Rubio-Bollinger, H. Suderow, and S. Vieira, Phys. Rev. Lett. **86**, 5582 (2001).
[7] E. A. Yelland, J. R. Cooper, A. Carrington, N. E. Hussey, P. J. Meeson, S. Lee, A. Yamamoto, and S. Tajima, Phys. Rev. Lett. **88**, 217002 (2002).
[8] R. Cubitt, M. R. Eskildsen, C. D. Dewhurst, J. Jun, S. M. Kazakov, and J. Karpinski, Phys. Rev. Lett. **91**, 047002 (2003).
[9] A. Gurevich and V. M. Vinokur, Phys. Rev. Lett. **90**, 047004 (2003).
[10] Y. Tanaka, Phys. Rev. Lett. **88** 017002 (2002).
[11] P. C. Canfield, P. L. Gammel, and D. J. Bishop, Phys. Today **51** (10), 40 (1998).
[12] S. V. Shulga, S.-L. Drechsler, G. Fuchs, K.-H. Müller, K. Winzer, M. Heinecke, and K. Krug, Phys. Rev. Lett. **80**, 1730 (1998).
[13] Q. Yuan and P. Thalmeier, Phys. Rev. B **68**, 174501 (2003); also, for example, K. Maki, P. Thalmeier, and H. Won, *ibid.* **65**, 140502 (2002).
[14] T. Yokoya, T. Kiss, T. Watanabe, S. Shin, M. Nohara, H. Takagi, and T. Oguchi, Phys. Rev. Lett. **85**, 4952 (2000).
[15] E. Boaknin, R. W. Hill, C. Proust, C. Lupien, L. Taillefer, and P. C. Canfield, Phys. Rev. Lett. **87**, 237001 (2001).
[16] K. Izawa, A. Shibata, Y. Matsuda, Y. Kato, H. Takeya, K. Hirata, C. J. van der Beek, and M. Konczykowski, Phys. Rev. Lett. **86**, 1327 (2001).
[17] P. Martínez-Samper, H. Suderow, S. Vieira, J. P. Brison, N. Luchier, P. Lejay, and P. C. Canfield, Phys. Rev. B **67**, 014526 (2003).
[18] I. K. Yanson, V. V. Fisun, A. G. M. Jansen, P. Wyder, P. C. Canfield, B. K. Cho, C. V. Tomy, and D. McK. Paul, Phys. Rev. Lett. **78**, 935 (1997).
[19] S. B. Dugdale, M. A. Alam, I. Wilkinson, R. J. Hughes, I. R. Fisher, P. C. Canfield, T. Jarlborg, and G. Santi, Phys. Rev. Lett. **83**, 4824 (1999).
[20] J. Zarestky, C. Stassis, A. Goldman, P. Canfield, G. Shirane, and S. Shapiro, Phys. Rev. B **60**, 11 932 (1999).
[21] T. Dahm and N. Schopohl, Phys. Rev. Lett. **91**, 017001 (2003).
[22] L. Glémot, J. P. Brison, J. Flouquet, A. I. Buzdin, I. Sheikin, D. Jaccard, C. Thessieu, and F. Thomas, Phys. Rev. Lett. **82**, 169 (1999).
[23] V. G. Kogan, Phys. Rev. B **66**, 020509 (2002); S. L. Budko and P. C. Canfield, *ibid.* **65**, 212501 (2002).
[24] U. Welp, A. Rydh, G. Karapetrov, W. K. Kwok, G. W. Crabtree, Ch. Marcenat, L. Paulius, T. Klein, J. Marcus, K. H. P. Kim, C. U. Jung, H.-S. Lee, B. Kang, and S.-I. Lee, Phys. Rev. B **67**, 012505 (2003).
[25] L. Lyard, P. Samuely, P. Szabo, T. Klein, C. Marcenat, L. Paulius, K. H. P. Kim, C. U. Jung, H.-S. Lee, B. Kang, S. Choi, S.-I. Lee, J. Marcus, S. Blanchard, A. G. M. Jansen, U. Welp, G. Karapetrov, and W. K. Kwok, Phys. Rev. B **66**, 180502(R) (2002).
[26] B. Kang, H.-J. Kim, H.-S. Lee, and Sung-Ik Lee, cond-mat/0403455 (unpublished).
[27] R. H. T. Wilke, S. L. Bud'ko, P. C. Canfield, D. K. Finnemore, R. J. Suplinskas, and S. T. Hannahs, Phys. Rev. Lett. **92**, 217003 (2004).
[28] A. A. Golubov and I. I. Mazin, Phys. Rev. B **55**, 15 146 (1997); A. A. Golubov and A. E. Koshelev, *ibid.* **68**, 104503 (2003).
[29] S. Lee, H. Mori, T. Masui, Y. Eltsev, A. Yamamoto, and S. Tajima, J. Phys. Soc. Jpn. **70**, 2255 (2001).
[30] S. Deemyad, T. Tomita, J. J. Hamlin, B. R. Beckett, J. S. Schilling, D. G. Hinks, J. D. Jorgensen, S. Lee, and S. Tajima, Physica C **385**, 105 (2002).

[31] A. F. Goncharov and V. V. Struzhkin, Physica C **385**, 117 (2002).
[32] M. Prohammer and E. Schachinger, Phys. Rev. B **36**, 8353 (1987).
[33] A. F. Goncharov, V. V. Struzhkin, E. Gregoryanz, JingzhuHu, R. J. Hemley, H. K. Mao, G. Lapertot, S. L. Bud'ko, and P. C. Canfield, Phys. Rev. B **64**, 100509 (2001).
[34] T. Tomita, J. J. Hamlin, J. S. Schilling, D. G. Hinks, and J. D. Jorgensen, Phys. Rev. B **64**, 092505 (2001).
[35] T. Masui, S. Lee, and S. Tajima, Physica C **383**, 299 (2002); Phys. Rev. B **70**, 024504 (2004).
[36] K. P. Meletov, M. P. Kulakov, N. N. Kolesnikov, J. Arvanitidis, and G. A. Kourouklis, JETP Lett. **75**, 406 (2001).
[37] E. Alleno, J. J. Neumeier, J. D. Thompson, P. C. Canfield, and B. K. Cho, Physica C **242**, 169 (1995).
[38] I. I. Mazin and V. P. Antropov, Physica C **385**, 49 (2003).